Available online at www.sciencedirect.com
SCIENCE DIRECT
Journal of Photochemistry and Photobiology A: Chemistry 180 (2006) 59–64
Journal of Photochemistry and Photobiology A:Chemistry
www.elsevier.com/locate/jphotochem

The photoluminescence of rhodamine B encapsulated in mesoporous Si-MCM-48, Ce-MCM-48, Fe-MCM-48 and Cr-MCM-48 molecular sieves

Yaofeng Shao [a], Lingzhi Wang [a], Jinlong Zhang [a,*], Masakazu Anpo [b]

[a] *Laboratory for Advanced Materials and Institute of Fine Chemicals, East China University of Science and Technology, 130 Meilong Road, Shanghai 200237, People's Republic of China*
[b] *Graduate School of Engineering, Osaka Prefecture University, 1-1 Gakuen-cho, Sakai, Osaka 599-8531, Japan*

Received 18 July 2005; received in revised form 30 August 2005; accepted 21 September 2005
Available online 21 October 2005

Abstract

Photophysical and photochemical properties of rhodamine B molecules encapsulated into various mesoporous molecular sieves were investigated by absorption and emission spectra and fluorescence decay. The different fluorescence properties were observed within different RhB/Me-MCM-48 (Me = Ce, Fe, Cr) composites. There were larger blue shifts in fluorescence spectra when RhB included in Ce-MCM-48 than that in Fe-MCM-48 and Cr-MCM-48. However, the much larger electron transfer efficiencies from excited dye molecules to iron and chromium oxide occurred within the system of RhB/Fe-MCM-48 and RhB/Cr-MCM-48 than that within the system of RhB/Ce-MCM-48. The effects of Ce-containing amounts on the fluorescence properties were also investigated in detail.
© 2005 Elsevier B.V. All rights reserved.

Keywords: MCM-48; Me-MCM-48; Fluorescence; Rhodamine B; Electron transfer

1. Introduction

Photoinduced electron transfer in heterogeneous hosts with various dyes has been studied extensively with reference to solar energy utilization [1]. Especially, laser dyes have been included in solid matrixes such as minerals [2], polymers [3], sol–gel hosts [4] and porous inorganic materials in order to increase their photostability [5]. MCM-48, a mesoporous molecular sieve, invented by Mobil [6,7] in 1992, has attracted considerable attention because of its high surface area, three-dimensional channel, ordered pore structure array, and narrow pore size distribution. The MCM-48 materials with these unique properties have promising utility for incorporation of large organic molecules to improve the efficiency of photoelectricity conversion and study the photophysical and photochemical properties about organic molecules incorporated in host. In addition, the tetrahedral Si (IV) in the Si-MCM-48 framework can be replaced by other metal ions such as Al (III), Ti (IV), Mn (II), and other transition metal ions [8–10]. This makes it possible to modify the Si-MCM-48 framework to enhance the electron transfer efficiency of incorporated molecules such as rhodamine B (RhB), which is one of the most readily available and useful reagents for use as an organic laser dye with a higher absorption coefficient and fluorescence yield for collecting and utilizing photoenergy [11,12].

In this paper, we report the encapsulation of rhodamine B into the three-dimensional channels of Si-MCM-48 and Ce-MCM-48, Fe-MCM-48, Cr-MCM-48. We study in detail the effect of Si-MCM-48, Ce-MCM-48, Fe-MCM-48 and Cr-MCM-48 on the photophysical and photochemical properties of rhodamine B through absorption and fluorescence spectra. In addition, we demonstrated the fluorescence properties of rhodamine B in Ce-MCM-48 with different cerium contents. In a word, study on their photoluminescence in MCM-48 and Me-MCM-48 (Me = Ce, Fe, Cr) may provide useful information for taking advantage of solar energy.

* Corresponding author. Tel.: +86 21 64252062; fax: +86 21 64252062.
E-mail address: jlzhang@ecust.edu.cn (J. Zhang).

1010-6030/$ – see front matter © 2005 Elsevier B.V. All rights reserved.
doi:10.1016/j.jphotochem.2005.09.018

2. Experimental section

2.1. Synthesis of molecular sieves Si-MCM-48 and Me-MCM-48 (Me = Ce, Fe, Cr)

The Si-MCM-48 molecular sieves were prepared as follows: 10 mL of tetraethylorthosilicate (TEOS) was mixed with 50 mL of deionized water and the mixture was vigorously stirred for 40 min, then 0.9 g of NaOH solution was added into mixture. After another 60 min of vigorously stirring, 10.61 g of cetyltrimethylammonium bromide (CTAB) was added to the mixture and continued stirring for 60 min. The typical composition of final gel mixture was 1.0TEOS:0.65CTAB:0.5NaOH:62H_2O. The mixture was heated for 72 h at 393 K in an autoclave under static condition, the resulting MCM-48 product was filtered, washed with distilled water and dried at 373 K. The as-synthesized samples were then calcined for 4 h at 550 °C, after increasing the temperature to 550 °C at 1 °C/min of heating rate.

The Me-MCM-48 (Me = Ce, Fe, Cr) was synthesized by the same procedure used for Si-MCM-48 except that the required Ce $(NO_3)_3 \cdot 6H_2O$, Fe $(NO_3)_3 \cdot 9H_2O$, $Cr(NO_3)_3 \cdot 9H_2O$, which as Ce, Fe, Cr source, respectively, added after the NaOH was added completely.

2.2. Inclusion of rhodamine B into Si-MCM-48 and Me-MCM-48 (Me = Ce, Fe, Cr)

Calcined Si-MCM-48, Ce-MCM-48, Fe-MCM-48, Cr-MCM-48 molecular sieves (100 mg) were heated at 200 °C for 6 h to remove water adsorbed on the surface, then at once transferred to a flask and allowed to cool to room temperature under N_2 atmosphere. Rhodamine B ($5\,mL \times 10^{-5}$ M; shown in Scheme 1) aqueous solution was added into the flask; after 24 h, the solids were filtered and washed thoroughly with the solvents until the solution was clear, which indicated that the dye molecules attached to the external surface of Si-MCM-48, Ce-MCM-48, Fe-MCM-48, Cr-MCM-48 have been removed. Then the samples were dried for characterization.

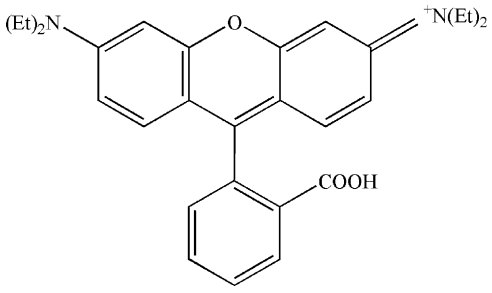

Scheme 1. The molecular structure of rhodamine B (RhB).

2.3. Characterization

X-ray power diffraction (XRD) patterns of all samples were recorded on Rigaku D/MAX-2550 diffractometer using Cu Ka radiation of wavelength 1.541 Å. The diffuse reflectance UV–vis spectra were recorded with VARIAN Cary 500. The fluorescence spectra of all samples were recorded with Cary Eclipse fluorescence spectrophotometer. The decay curves were recorded on Edinburgh F 900 fluorescence lifetime spectrometer. The lifetimes were calculated from the decay curves by using the least-square method. All the above measurements were carried out at room temperature.

3. Results and discussion

3.1. XRD analysis

Powder XRD patterns of calcined Si-MCM-48, Me-MCM-48 (Me = Ce, Fe, Cr) and Ce-MCM-48 with different Ce-doped contents are shown in Fig. 1. As Fig. 1(a) shown that all materials exhibit eight distinguishable Bragg peaks that can be indexed to different (*h k l*) reflections. These reflections verify the presence of cubic phase (*Ia3d*) with well crystallinity and high long-range order and no impurity phase is detected. Fig. 1(b) also shows the diffraction peaks of *Ia3d* cubic structure, which indicating that the long-range order MCM-48 were synthesized. Fig. 1(b) shows that the intensities of the XRD peaks of Ce-MCM-48 with different Ce contents decrease with the Ce content increasing in the samples, suggesting that the mesoporous structures

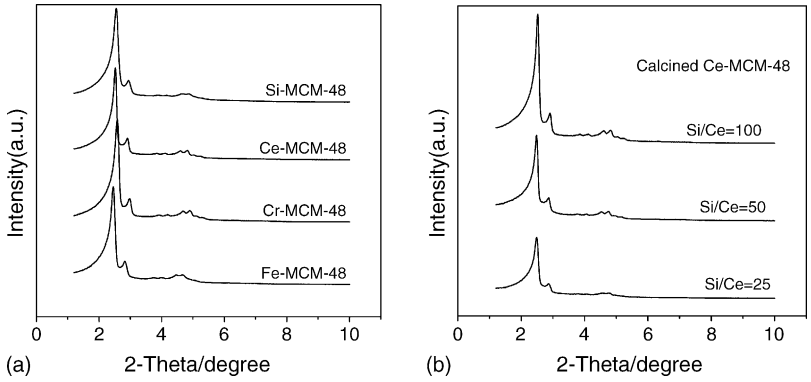

Fig. 1. (a) Powder XRD patterns of calcined Si-MCM-48, Ce-MCM-48, Cr-MCM-48, Fe-MCM-48 with a Si/Me of 100 (Me = Ce, Cr, Fe); (b) powder XRD patterns of Ce-MCM-48 with different Ce-doped contents.

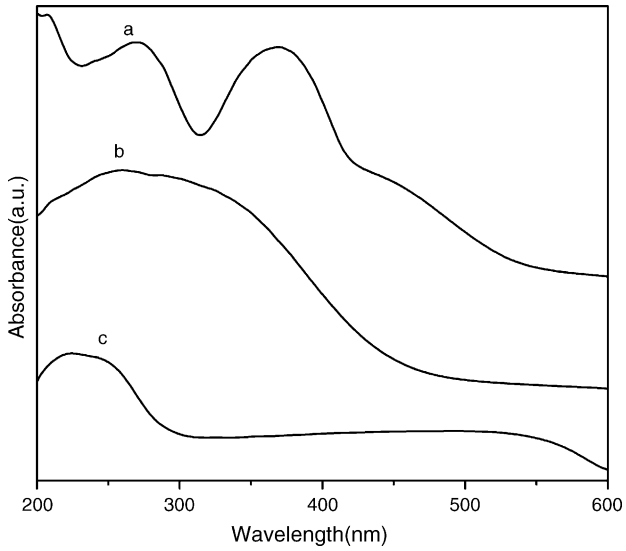

Fig. 2. Diffuse reflectance UV–vis spectra of calcined (a) Cr-MCM-48, (b) Ce-MCM-48, (c) Fe-MCM-48 with a Si/Me of 100 (Me = Ce, Cr, Fe).

of Ce-MCM-48 become less uniform upon the introduction of Ce into the framework and the cubic lattice is destroyed. The contents of cerium in the present samples are not quantified and just the values calculated from the raw materials.

3.2. Diffuse reflectance UV–vis spectroscopy

The diffuse reflectance UV–vis spectroscopy is known to be a very sensitive probe for the identification and characterization of metal ion coordination and its existence in the framework and/or in the extraframework position of metal containing zeolites and mesoporous materials. Fig. 2 depicts the UV spectra of the calcined Ce-MCM-48, Cr-MCM-48, Fe-MCM-48 samples. The Ce-MCM-48 sample shows a single peak with a maximum at 300 nm. The position of ligand to metal charge transfer ($O^{2-} \rightarrow Ce^{4+}$) spectra depends on the ligand field symmetry surrounding the Ce center. The electronic transitions from oxygen to cerium require higher energy for a tetracoordinated Ce^{4+} than for a hexa-coordinated one [13]. Therefore, it may be inferred that the absorption band centered at 300 nm for Ce-MCM-48 samples is due to the presence of one type of well-dispersed Ce^{4+} species (presumably in a tetra-coordinated environment). The Fe-MCM-48 sample shows a strong absorption in the 200–300 nm region (a clearly distinguished peak at $\lambda = 225$ nm) attributed to the charge-transfer (CT) transitions involving isolated framework Fe_3^+ in $(FeO)_4^-$ tetrahedral geometry [14]. The Cr-MCM-48 sample shows two peaks around 370 and 272 nm, the latter being relatively broad, it indicates that two intense $O \rightarrow Cr^{6+}$ charge transfer bands of a chromate species are dominated in the calcined Cr-MCM-48 [15].

3.3. Fluorescence spectra

In this paper, the emission spectra are obtained by exciting at respective maximum excitation wavelength.

Fig. 3(a) shows the absorption of RhB in aqueous solution and Si-MCM-48, Ce-MCM-48, Fe-MCM-48, Cr-MCM-48. Compared with absorption in aqueous solution, the absorption within Si-MCM-48 and Ce-MCM-48, Fe-MCM-48, Cr-MCM-48 barely shows shoulder peak at about 525 nm. It indicates that the RhB molecules mainly exist in a monomer form within mesoporous materials due to its high surface area [16]. According to Fig. 3(b), it can be known that the maximum emission of RhB in aqueous solution at about 581 nm, and the peak of the fluorescence spectra of RhB in the Si-MCM-48 at around 586 nm, which red shifting 6 nm compared with that in aqueous solution. This result is attributed to the reduction of the HOMO–LUMO band gap caused by the confinement effect [17], when RhB dyes are incorporated into MCM-48, the HOMO and LUMO energy levels all increase due to the confinement effect, but the HOMO energy increases more than that of LUMO, so the HOMO–LUMO band gap reduces compared with that in solution [18], resulting in the red shift of absorption spectra. Meanwhile, the intensity of maximum emission of RhB in Si-MCM-48 distinctly decreases compared with that in aqueous solution. It can be explained by the interaction between dye molecules and silanols groups on the surface of MCM-48, which resulting in the energy transfer from excited state of RhB to MCM-48 so that increasing the non-radiated transition of dye-excited state and decreasing the fluorescence emission [19]. Fig. 3(b) also shows that compared with that in aqueous solution and Si-MCM-48, the blue shifts are observed in doped metal ions Me-MCM-48 (Me = Ce, Fe, Cr), at the same time, the intensities

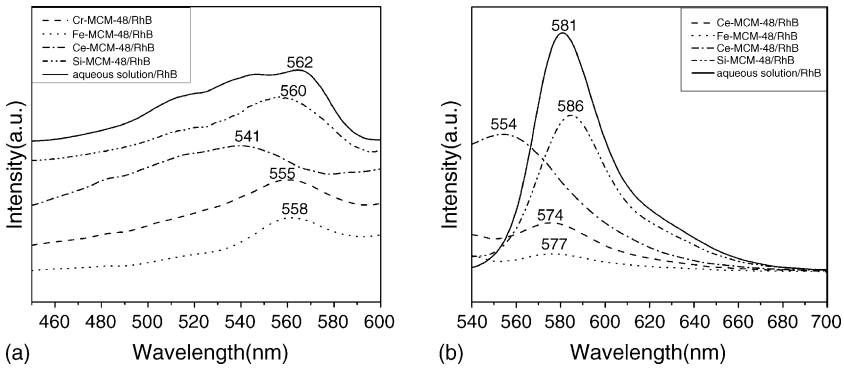

Fig. 3. Absorption (a) and emission (b) spectra of RhB in aqueous solution at $\lambda_{ext} = 562$ nm, Si-MCM-48 at $\lambda_{ext} = 560$ nm, Ce-MCM-48 at $\lambda_{ext} = 541$ nm, Fe-MCM-48 at $\lambda_{ext} = 558$ nm and Cr-MCM-48 at $\lambda_{ext} = 555$ nm.

Table 1
Relative quantum yields s (slopes of intensity vs. dye content plots)[a] of rhodamine B (RhB) in various mesoporous materials

Numbers	RhB in various mesoporous materials	s (ppm^{-1})
1	Si-MCM-48/RhB	2.5
2	Ce-MCM-48/RhB	2.2
3	Cr-MCM-48/RhB	0.91
4	Fe-MCM-48/RhB	0.34
5	1% Ce-MCM-48/RhB	2.2
6	2% Ce-MCM-48/RhB	1.16
7	4% Ce-MCM-48/RhB	1.63

[a]Reference to [21].

of the fluorescence spectra of RhB in Me-MCM-48 all decrease at different degrees compared with that in aqueous solution and Si-MCM-48. These results indicate that the RhB molecules interact with framework Ce^{4+}, Fe^{3+}, Cr^{6+}. It is also found that the maximum emission of RhB in Ce-MCM-48 blue shifts about 30 nm compared with that in aqueous solution, however, the blue shifts are only 4 and 7 nm in Fe-MCM-48 and Cr-MCM-48, respectively. This result indicates that the isolated tetrahedrally coordinated cerium oxide moieties in the mesopores have a strong interaction with RhB molecules to be effective in anchoring RhB molecules in a highly dispersed state. Therefore, the strong interaction of RhB organic molecule with isolated framework Ce^{4+} should be coordinated. The π-conjugation is changed because of the interaction of RhB with Ce^{4+}, and the transition energy increases with a decrease of π-conjugation, so the maximum emission of RhB has a large blue shift [20]. However, the maximum emission of RhB in Cr-MCM-48 and in Fe-MCM-48 only blue shifts 4–7 nm, it can be explained by the weak coordination between Fe^{3+}, Cr^{6+} and RhB. On the other hand, the intensities of fluorescence spectra of RhB in Cr-MCM-48 and in Fe-MCM-48 are much lower than that in Si-MCM-48 and aqueous solution. In addition, the relative quantum yields of rhodamine B in various mesoporous materials are listed in Table 1. The relative quantum yields are expressed as s, the slopes of plots of fluorescence intensity versus the RhB content in ppm [21]. It can be seen that the relative quantum yield of RhB in MCM-48 decreases in the following order Si-MCM-48 > Ce-MCM-48 > Cr-MCM-48 > Fe-MCM-48. This result is due to the higher electron transfer efficiency between metal ions (Fe^{3+}, Cr^{6+}) and RhB than that with rare earth ion (Ce^{4+}). Das et al. [22] also proved that iron and chromium were efficient quenchers.

Fig. 4 shows the changes in the intensity and peaks of fluorescence emission and fluorescence excitation spectra of RhB encapsulated in Ce-MCM-48 doped with different contents of cerium and Ce-MCM-48 without RhB encapsulated. It can be seen that the Ce-MCM-48 without RhB encapsulated has not fluorescence emission and excitation spectra. It was found that the maximum emission intensities of RhB firstly decrease with the cerium content increasing, then increase with the cerium content increasing. In addition, the relative quantum yields of rhodamine B in Ce-MCM-48 doped with different contents of cerium are listed in Table 1. From Table 1, it can be seen that the relative quantum yield of RhB in different Ce-containing Ce-MCM-48 decreases in the following order 1% Ce-MCM-48 > 4% Ce-MCM-48 > 2% Ce-MCM-48. It can be explained that the electron transfer efficiency from excited dye molecules to electron acceptors (Ce^{4+}) increases with the cerium content doped increasing, which quenched the fluorescence of dye molecules [23,24]. However, on the other hand, the more of isolated framework Ce^{4+}, the more of RhB molecules introduced into the channels of molecular sieves, so the intensity of emission and relative quantum yield increase with the cerium content doped increasing. Therefore, because of the above two combination effects, the relative quantum yield and intensity of RhB in 2% Ce-MCM-48 is lower than that in 1% Ce-MCM-48 and 4% Ce-MCM-48. At the same time, the blue shifts of maximum emission of RhB also increase with the cerium content doped increasing. The maximum emission of RhB blue shifts only 27 nm in 1% Ce-MCM-48 compared with that in aqueous solution, however, it blue shifts about 51 nm in 2% Ce-MCM-48 compared with that in aqueous solution, but it only blue shifts another 2 nm in 4% Ce-MCM-48. These results can be explained by the following reasons: most of the Ce atoms in the Ce-MCM-48 samples occupy site-isolated positions within the silica framework, except for high Ce content samples. The highly dispersed tetra-coordinated Ce^{4+} species play an important role of effective adsorption sites. At the local areas of microenvironment, the number of framework Ce^{4+} ions is increased with the

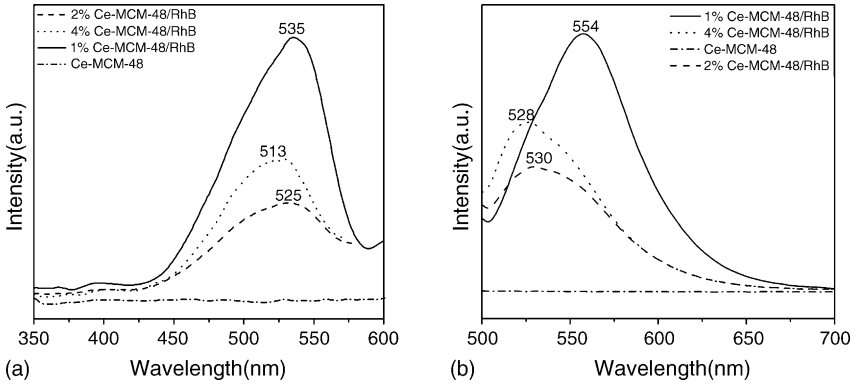

Fig. 4. Excitation (a) and emission (b) spectra of RhB in Ce-MCM-48 with different cerium contents and Ce-MCM-48 without RhB incorporation. The excitation wavelength was 535 nm for 1% Ce-MCM-48/RhB, 525 nm for 2% Ce-MCM-48/RhB, 513 nm for 4% Ce-MCM-48/RhB, respectively.

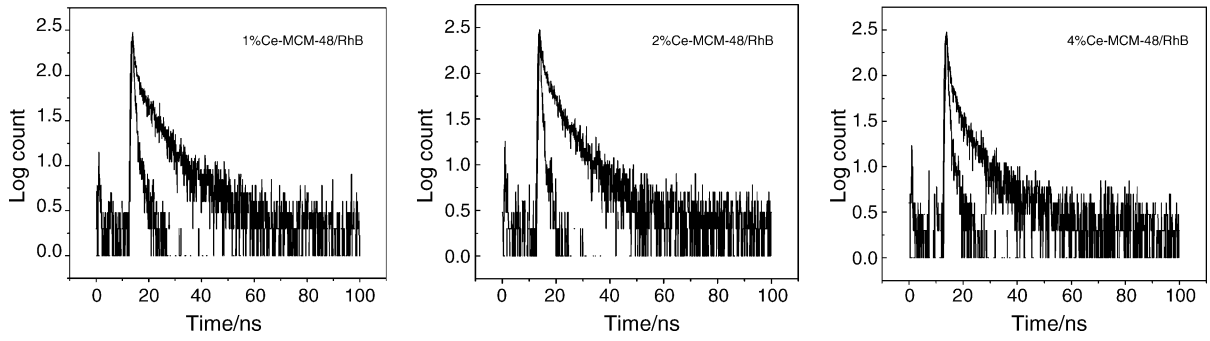

Fig. 5. Fluorescence decay profiles of RhB in Ce-MCM-48 with different cerium contents.

Table 2
The fluorescence data of RhB in Ce-MCM-48

Host	τ_1(ns)	τ_2(ns)	χ^2
1% Ce-MCM-48	0.17	10.42	1.033
2% Ce-MCM-48	0.80	7.68	1.056
4% Ce-MCM-48	0.75	7.66	1.081

content of doped Ce increasing. Therefore, the more numbers of framework Ce^{4+} ions coordinate with single RhB molecule, the larger decrease of π-conjugation is occurred. The blue shifts of maximum emission of RhB increase with the cerium content increasing. However, when the content of cerium doped increases to 2%, the number of framework Ce^{4+} ions has reached saturation at the local areas. Continuing to increase the content of cerium doped, the blue shift barely increases.

3.4. Fluorescence lifetime

Fig. 5 shows that all RhB in Ce-MCM-48 are found to exhibit biexponential decay, irrespective of the content of cerium 1, 2 and 4%. The two lifetimes are designated as τ_1 (short) and τ_2 (long). Kano et al. [25] suggest that two types of existing state, in solution and absorbed on surface, account for the biexponential decay. Similarly, two types of absorbing state may interpret our results: (i) RhB molecules absorb on the isolated surface Ce^{4+} site and (ii) RhB molecules absorb on the silanol site. For the (i) form, the RhB molecules are tightly fixed and become more rigid, moreover electron transfer from the RhB molecules to the d orbit of Ce existed, so the excited state of the (i) form is more stable than that of the (ii) form, namely, the τ_1 belongs to (ii) form and τ_2 belongs to (i) form. In addition, Table 2 shows that the lifetime gradually decreases with the increasing of content of cerium doped into MCM-48. It also could verify the explanation ahead (Fig. 4 and Table 1) that the electron transfer efficiency from excited dye molecules to the electron acceptors (Ce^{4+}) increases with the cerium content increasing, which quenched the fluorescence of dye molecules.

4. Conclusion

Rhodamine B molecules were successfully introduced into the channels of Si-MCM-48 and Me-MCM-48 (Me = Ce, Fe, Cr). The absorption spectra indicated the Rhodamine B molecules mainly existed in monomer form within MCM-48 and Me-MCM-48, which avoided the aggregation of dye molecules. The fluorescence results showed that the electron transfer from excited dye molecules to the cerium, iron and chromium oxide occurred within the system of RhB/Me-MCM-48. It also showed the electron transfer efficiencies between RhB and iron, chromium ions were much higher than that between RhB and cerium ion. In addition, the maximum emission of RhB molecules within Ce-MCM-48 showed the larger blue shift than that within Fe-MCM-48 and Cr-MCM-48. This result indicated the coordination effect of dye molecules with Ce^{4+} ions was much higher than that of dye molecules with Fe^{3+} and Cr^{6+} ions. It was also found that the blue shift of maximum emission of RhB within Ce-MCM-48 increased with the cerium content increasing. However, the lifetime of RhB within Ce-MCM-48 decreased with the cerium content increasing.

Acknowledgements

This work have been supported by Program for New Century Excellent Talents in University (NCET-04-0414); Shanghai Nanotechnology Promotion Center (0452nm010); National Basic Research Program of China (2004CB719500).

References

[1] K. Kalyanasundaram, Photochemistry in Microheterogeneous Systems, Academic, New York, 1997.
[2] R. Hoppe, A. Ortlam, J. Rathousky, G. Schulz-Ekloff, A. Zukal, Micropor. Mater. 8 (1997) 267.
[3] G. Somasundaram, A. Ramalingam, J. Photochem. Photobiol. A. 125 (1999) 93.
[4] S.K. Lam, D. Lo, Chem. Phys. Lett. 281 (1997) 35.
[5] H. Nishiguchi, K. Yukawa, H. Yamashita, Anpo.F M., J. Photochem. Photobiol. A. 99 (1995) 1.
[6] C.T. Kresge, M.E. Leonowicz, W.J. Roth, J.C. Vartuli, J.S. Beck, Nature 359 (1992) 710.
[7] J.S. Beck, J.C. Vartuli, W.J. Roth, M.E. Leonowicz, C.T. Kresge, K.D. Schmitt, C.T.W. Chu, D.H. Olson, E.W. Sheppard, S.B. McCullen, J.B. Higgins, J.L. Schlenker, J. Am. Chem. Soc. 114 (1992) 10834.
[8] A. Griselda, Liliana.B. Eimer, Gustavo.A. Pierella, Oscar.A. Monti, Anunziata, Catal. Lett. 78 (2002) 65.
[9] J. Xu, Z. Luan, M. Hartmann, L. Kevan, Chem. Mater. 11 (1999) 2928.
[10] M. Morey, A. Davidson, G. Stucky, Micropor. Mater. 6 (1996) 99.
[11] A. Makiihima, T. Tani, J. Am. Ceram. Soc. 69 (1986) 72.
[12] J.M. McKiernan, S.A. Yamanaka, B. Dunn, J.I. Zink, J. Phys. Chem. 94 (1990) 5652.

[13] M.D. Kadgaonkara, S.C. Lahaa, R.K. Pandeyb, P. Kumarb, S.P. Mirajkara, R. Kumar, Catal. Today 97 (2004) 225.
[14] T. Inui, H. Nagata, M.J. Inoue, J. Catal 139 (1993) 482.
[15] B.M. Weckhuysen, A.A. Verberckmoes, A.R. De Baets, R.A. Schoonheydt, J. Catal. 166 (1997) 160.
[16] H. Nishikiori, T. Fujii, J. Phys. Chem. B 101 (1997) 3680.
[17] F. Marquez, H. Garcý, E. Palomares, L. Fernandez, A. Corma, J. Am. Chem. Soc. 122 (2000) 6520.
[18] L.Z. Zhang, P. Cheng, G.Q. Tang, D.Z. Liao, J. Lumin. 104 (2003) 123.
[19] Y. Gao, T.A. Konovalova, J.N. Lawrence, M.A. Smitha, J. Nunley, R. Schad, J. Phys. Chem. B 107 (2003) 2459.
[20] D.M. Li, J.L. Zhang, M. Anpo, Dyes Pigments 63 (2004) 71.
[21] H.J. Buschmann, T. Wolff, J. Photochem. Photobiol. A: Chem. 121 (1999) 99.
[22] S.N. Das, M. Panda, Asian J. Spectrosc. 7 (2003) 87.
[23] S.E. Gunter, W. Dieter, V.D. Bast, A. Robert, Micropor. Mesopor. Mater. 51 (2002) 91.
[24] W.J. Zhao, D.M. Li, B. He, J.L. Zhang, J.Z. Huang, L.Z. Zhang, Dyes Pigments 64 (2005) 265.
[25] K. Kano, T. Miyake, K. Uomoto, T. Sato, T. Ogawa, S. Hashimoto, Chem. Lett. 144 (1983) 1867.